

An integral equation approach to an sp^3d^5 liquid: electronic structure of liquid silicon

This article has been downloaded from IOPscience. Please scroll down to see the full text article.

2000 J. Phys.: Condens. Matter 12 1667

(<http://iopscience.iop.org/0953-8984/12/8/309>)

View [the table of contents for this issue](#), or go to the [journal homepage](#) for more

Download details:

IP Address: 171.66.16.218

The article was downloaded on 15/05/2010 at 20:17

Please note that [terms and conditions apply](#).

An integral equation approach to an sp^3d^5 liquid: electronic structure of liquid silicon

Monika S K Fuchs†

Institute of Technical Physics, DLR Stuttgart, Pfaffenwaldring 38-40, 70569 Stuttgart, Germany

Received 26 October 1999

Abstract. In order to combine the advantages of tight-binding integral equation methods with basis sets not restricted to the lowest two orbital quantum numbers we extend the molecular fluid approach for the sp^3 model of Lomba *et al* to arbitrarily high orbital quantum numbers. As an example, we present a single-superchain/effective-medium calculation of the electronic density of states for liquid silicon within a tight-binding approximation that includes, besides the 3s and 3p orbitals, also the 3d orbitals. Comparison with results from the sp^3 model and different molecular dynamics results shows that within this sp^3d^5 model very good agreement with plane-wave calculations is found whereas the sp^3 model leads to unsatisfactory results.

1. Introduction

The so-called integral equation or effective-medium methods are long-standing approaches to the electronic structure of liquids [1–3]. However, in the early formulation only simple model systems could be handled. The interest of theorists in liquid matter grew in the last decade when the enormous increase of computational capacity enabled us to describe realistic materials. Typically, atomic and sometimes electronic structures of various liquid materials are determined by molecular dynamics (MD) or Monte Carlo (MC) simulations. Nevertheless, real *ab initio* calculations are still very time consuming and are done only for some molten metals and alloys (see, e.g., [4] and references therein) and a few more covalent (e.g., silicon [5–7], others [8–11]) or ionic [12] materials. To a large extent, MD simulations with empirical pair potentials are performed to determine atomic structures (e.g., for silicon [13–18]). Electronic structures are calculated most often by means of a tight-binding basis [19–22]. The reason for this is that the set-up and diagonalization of the (large) Hamiltonian has to be done for many steps of the simulation and, therefore, is a time-consuming factor which can be reduced in impact by the use of a small (e.g., tight-binding) basis set instead of a more complete one (e.g., plane waves).

Beyond the huge computational effort, statistical methods like MD and MC simulations have a further disadvantage: the statistical fluctuations can make it difficult to decide whether a feature—for instance, in the electronic density of states (DOS)—is a physical phenomenon or an artifact of statistical noise (e.g., a slight dip at the Fermi energy [20, 22]). This problem is aggravated by the fact that due to the computational cost the statistical ensemble is not very large. In this case, integral equation methods like the single-superchain/effective-medium approximation (SSCA/EMA) are a good alternative or supplement to MD simulations for the

† Present address: Technische Universität München, Lehrstuhl für Theoretische Chemie, Lichtenbergstrasse 4, 85747 Garching, Germany.

following reasons: (i) they include no statistical fluctuations; (ii) they are relatively low cost in computational time; and (iii), last but not least, it is shown that the SSCA/EMA agrees very well with analogous MD simulations [23, 24] and, therefore, contains only a negligible systematic error.

Although silicon is a prototype for an elemental semiconductor, in its liquid state—even if metallic—it is not a simple material. 1-Si has a coordination number less than 7 which is a very low value in comparison to those for typical metals where each atom has about 10–12 nearest neighbours. The covalency of the bonds is also stronger than in simple metals and the conductivity is relatively small. The need for understanding this covalent–metallic mixed material is a reason for increased theoretical examination. Beyond that, it represents a suitable example for carefully testing different simulation methods, models etc.

In the tight-binding picture, liquid silicon is most often reduced to a model that includes only 3s and 3p states, whereas even the minimal basis set of Si introduced by Ching [25] includes also the 3d states. Molecular dynamics (MD) simulations going beyond this sp^3 model (i.e. with plane waves [7] or in the sp^3d^5 model [20]) are computationally very time consuming. The above-mentioned problem of statistical fluctuations leads to the question of whether there is a dip at the Fermi energy or not [20]. In the first case, this would mean that the remainder of the covalency is large enough to affect the electronic structure in a relevant manner.

Although SSCA/EMA calculations are less time consuming, they have still been performed only for an sp^3 model [24]. In order to combine the advantages of the integral equation method with a less restricted basis set, we present a SSCA/EMA calculation of the electronic density of states of an sp^3d^5 model of liquid silicon. For that purpose, we extend in section 2 the sp^3 -fluid model of Lomba *et al* [26] to general orbital quantum numbers. The results for the sp^3d^5 model are discussed in section 3.

2. SSCA/EMA formalism for multiband systems with general orbital symmetry

The equations of the SSCA/EMA are very similar to those known for the determination of the atomic structure of a liquid (e.g., hypernetted-chain or Percus–Yevick approximation). Independent of the special different closure relations, an Ornstein–Zernike (-like) equation occurs in all those approximations. This equivalence as well as the similar geometry of p-like orbitals and molecules of linear shape leads to the idea of the ‘molecular fluid approach’ treated in the following subsection.

For a detailed description of the formulae of the SSCA/EMA we refer the reader to the literature [26]. In the following we concentrate on the ideas that are important for an efficient handling of the angle dependence of the basis orbitals. Our notation follows reference [26].

2.1. Brief review of the molecular fluid approach

The SSCA/EMA can be derived from an infinite expansion of the Green’s function matrix elements in a tight-binding picture [27]. As a consequence, in the multiband SSCA/EMA, sums over all basis orbitals centred around one atom have to be built up. This can be formulated in terms of matrix multiplications. In particular, if an orbital quantum number l larger than zero (e.g., p orbitals) is included, it refers to a sub-matrix containing all allowed magnetic quantum numbers for that l . In the formulation of an sp^3 -fluid approach, Lomba *et al* use the convolution property

$$\int (\mathbf{A}\hat{s})(\hat{s}\mathbf{B}) \frac{d^2\hat{s}}{4\pi} = \frac{1}{3}\mathbf{A}\mathbf{B} \quad (1)$$

for the (sub-) matrices **A** and **B** to replace the sum over the magnetic quantum number μ of the p orbitals by the average over a newly introduced angular variable \hat{s} [26]. To simplify the notation, we use symbols like \hat{s} both as a unit vector and as the set of Euler angles describing its direction. Because in the following there remains always one rotational degree of freedom, the last of the three Euler angles can be chosen to be zero, so \hat{s} contains only one polar and one azimuthal angle.

The lhs of equation (1) has its counterpart in the theory of the atomic structure of the above-mentioned molecular fluids—by interpreting \hat{s} as the direction of the linearly shaped molecules. Assuming an isotropic fluid (i.e., no liquid crystal), one has to build up the average over all molecule orientations at every stage of the Ornstein–Zernike equation (see references [28,29]).

Returning to the sp^3 liquid, all angle-dependent tight-binding functions \mathcal{F} (these are the overlap S , transfer matrix elements V , ‘direct correlation’ C or ‘total correlation’ H) can be expanded, in general, in terms of rotational invariants ϕ (e.g., defined in [28]):

$$\mathcal{F}_{kl}(\mathbf{R}_{12}, \hat{s}_1, \hat{s}_2) = \sum_m F^{klm}(R_{12}) \phi^{klm}(\hat{s}_1, \hat{s}_2, \hat{\mathbf{R}}_{12}) \tag{2}$$

or more specifically, in a reference frame where the distance vector \mathbf{R}_{12} between the two atoms is parallel to the \hat{z} -axis, in terms of (totally normed) spherical harmonics Y :

$$\mathcal{F}_{kl}(\mathbf{R}_{12}, \hat{s}_1, \hat{s}_2) = 4\pi \sum_{\mu} F_{kl\mu}(R_{12}) Y_{\mu}^k(\hat{s}_1) Y_{-\mu}^l(\hat{s}_2) \tag{3}$$

where k and l are the orbital quantum numbers of the two orbitals involved. Analogous expansions hold for the Fourier transforms $\tilde{\mathcal{F}}(\mathbf{K}, \hat{s}_1, \hat{s}_2)$. We additionally present here the connection between the different sets of expansion coefficients (F^{klm} and $F_{kl\mu}$) because the original given in reference [26] contains an error:

$$F_{kl\mu} = \frac{1}{\sqrt{(2k+1)(2l+1)}} \sum_m m! \begin{pmatrix} k & l & m \\ 0 & 0 & 0 \end{pmatrix}^{-1} \begin{pmatrix} k & l & m \\ \mu & -\mu & 0 \end{pmatrix} F^{klm}$$

$$F^{klm} = \sqrt{(2k+1)(2l+1)} \frac{2m+1}{m!} \begin{pmatrix} k & l & m \\ 0 & 0 & 0 \end{pmatrix} \sum_{\mu} \begin{pmatrix} k & l & m \\ \mu & -\mu & 0 \end{pmatrix} F_{kl\mu}.$$

The same connection is valid for the coefficients of the Fourier transforms.

The main advantage of the expansion (2) is that it allows one to obtain the coefficients for the function in the three-dimensional Fourier space $\tilde{\mathcal{F}}^{klm}(K)$ from $F^{klm}(R)$ by a one-dimensional Fourier–Bessel transformation of order m [26,29].

2.2. Extension of the sp^3 -fluid model to general orbital quantum numbers

For using the method of Lomba *et al* [26] for orbital quantum numbers $l > 1$, some further extensions are needed. The first one is a generalization of the convolution property (1). The second one is a connection between the expansion coefficients $F_{kl\mu}(r)$ from (3) and the well known Slater–Koster parameters.

The meaning of the angular variable \hat{s} corresponding to the introduced new angular degree of freedom in reference [26] is very illustrative in the case of p-like orbitals: it describes the direction of the orbital. For d (or higher orbital quantum numbers), however, this seems not to hold because of the different shapes of the $d_{3z^2-r^2}$ and the $d_{x^2-y^2}$, d_{xy} etc orbitals. Anyway, if one deals only with $d_{3z^2-r^2}$ orbitals (or, in general, with the magnetic quantum number $\mu = 0$) in an arbitrary reference frame (\mathbf{r}') and defines \hat{s} as the z' -direction of that system in a fixed laboratory reference frame (\mathbf{r}), this spherical harmonic $Y_0^{l(\hat{s})}$ can be expressed as a linear combination of the spherical harmonics in the fixed laboratory system, where the coefficients

are given by the matrix elements of the rotation operator which contains the Euler angles $\alpha\beta\gamma$ and effects the transformation from one system to the other (see [30]):

$$Y_0^l(\hat{r}') = \sum_{\lambda=-l}^l \mathcal{D}_{\lambda 0}^{(l)}(\alpha, \beta, \gamma) Y_\lambda^l(\hat{r}) = \sum_{\lambda=-l}^l (-1)^\lambda \sqrt{\frac{4\pi}{2l+1}} Y_\lambda^l(\beta, \alpha) Y_\lambda^l(\hat{r}). \quad (4)$$

Because on the lhs only magnetic quantum numbers equal to zero are dealt with, the rhs is independent of the Euler angle γ . This allows us, as mentioned above, to choose the polar Euler angle γ to be zero. The remaining set of two independent angles α and β is the one describing the direction of \hat{s} . Note that the description of the reference frame by $\hat{z}' \parallel \hat{s}$ itself is not unequivocal. Only together with the demand that the last Euler angle vanishes is it free of its ambiguity.

Using the change of reference frame (4) one easily finds the following convolution property for the kernel of the angular projection on that orbital:

$$\int Y_0^{l*}(\hat{r}'_1(\hat{s})) Y_0^l(\hat{r}'_2(\hat{s})) \frac{d^2\hat{s}}{4\pi} = \frac{1}{2l+1} \sum_{\lambda=-l}^l Y_\lambda^{l*}(\hat{r}_1) Y_\lambda^l(\hat{r}_2) \quad (5)$$

where \hat{r}_1, \hat{r}_2 are unit vectors in the fixed laboratory system and \hat{r}'_1, \hat{r}'_2 are the *same* vectors in the reference system with $\hat{z}' \parallel \hat{s}$, so they depend on \hat{s} . Equation (5) is the general form of the convolution property (1) because the effect of the duplicate product with the \hat{s} on the lhs is nothing but that of a projector on the spherical harmonics for the p-like orbitals.

The connection between the expansion coefficients in equation (3) and the Slater–Koster parameters may be deduced in terms of the overlap integrals. We start from the two orbitals $\Phi_{\hat{s}_1}(\mathbf{r}_1)$ with angular dependence $Y_0^m(\hat{r}_1)$ in a reference system where $\hat{z}_1 \parallel \hat{s}_1$ and $\Psi_{\hat{s}_2}(\mathbf{r}_2)$ with the angular dependence $Y_0^n(\hat{r}_2)$ in a system where $\hat{z}_2 \parallel \hat{s}_2$. If Φ is centred around the origin and Ψ around \mathbf{R} and if we choose (without loss of generality) $\mathbf{R} \parallel \hat{z}$ of the fixed laboratory system, we obtain for these two orbitals and the overlap between them

$$\begin{aligned} \Phi_{\hat{s}_1}(\mathbf{r}) &= \varphi(r) \sum_{\mu=-m}^m \sqrt{\frac{4\pi}{2m+1}} (-1)^\mu Y_\mu^m(\hat{s}_1) Y_\mu^m(\hat{r}) \\ \Psi_{\hat{s}_2}(\mathbf{r}) &= \psi(|\mathbf{r}-\mathbf{R}|) \sum_{\nu=-n}^n \sqrt{\frac{4\pi}{2n+1}} (-1)^\nu Y_\nu^n(\hat{s}_2) Y_\nu^n(\widehat{\mathbf{r}-\mathbf{R}}) \\ \langle \Phi_{\hat{s}_1} | \Psi_{\hat{s}_2} \rangle &= \sum_{\mu=-m}^m \sum_{\nu=-n}^n \int d^3r \dots Y_\mu^{m*}(\hat{s}_1) Y_\nu^n(\hat{s}_2) Y_\mu^{m*}(\hat{r}) Y_\nu^n(\widehat{\mathbf{r}-\mathbf{R}}) \\ &= \sum_{\mu=-\min(m,n)}^{\min(m,n)} \frac{4\pi (-1)^\mu}{\sqrt{(2m+1)(2n+1)}} \langle \varphi Y_\mu^m | \psi Y_\mu^n \rangle Y_{-\mu}^m(\hat{s}_1) Y_\mu^n(\hat{s}_2) \end{aligned} \quad (6)$$

where $\langle \varphi Y_\mu^m | \psi Y_\mu^n \rangle$ is the well known Slater–Koster parameter $S_{nm\mu}^{\text{SK}}$ ($\mu = 0, 1, 2$ etc label σ, π, δ etc bonds). The sum over ν disappears because the terms with $\mu \neq \nu$ vanish. For the spherical harmonics we use the convention $Y_\mu^{m*} = (-1)^\mu Y_{-\mu}^m$ (e.g., from [30]). Comparing (3) and (6) one obtains immediately

$$S_{nm\mu} = \frac{(-1)^\mu}{\sqrt{(2m+1)(2n+1)}} S_{nm\mu}^{\text{SK}}. \quad (7)$$

The same connection between expansion coefficients and Slater–Koster parameters holds for the matrix elements of the Hamiltonian under the following assumptions:

- (i) No terms with three or more centres are included. This means that the potential occurring in the Hamiltonian consists of a sum of two atomic potentials, each centred around one of the atoms involved.
- (ii) The atomic potentials are spherically symmetric.

In this case, in the analogous deduction, only terms with modified radial functions (φ, ψ) occur (because the angular dependence given by the spherical harmonics is changed neither by the kinetic part of the Hamiltonian nor by an angle-independent potential). With the convolution property (5) one obtains the general form for the Ornstein–Zernike-like equation and the average diagonal Green’s function \bar{G} :

$$\tilde{H}_{jl\mu}(q) = \tilde{C}_{jl\mu}(q) + (-1)^\mu \rho \sum_{k \leq |\mu|} \tilde{H}_{jk\mu}(q)(2k+1)\bar{G}^k \tilde{C}_{kl\mu}(q) \quad (8)$$

$$z_l \bar{G}^l = 1 + 4\pi\rho \bar{G}^l \int_0^\infty \sum_{k,\mu} V_{lk\mu}(r)(2k+1)\bar{G}^k (-1)^{k+l} H_{kl\mu}(r)r^2 dr \quad (9)$$

where ρ is the particle density and $z_k = E - \varepsilon_k$ is the inverse of the diagonal Green’s function of the non-interacting system. The factor $2k + 1$ in equations (8) and (9) results from inserting the convolution property (5), whereas the sign $(-1)^\mu$ is a consequence of the expansion in terms of $Y_\mu Y_{-\mu}$ (equation (3)) instead of $Y_\mu Y_\mu^*$ (otherwise the factor $(-1)^\mu$ in equation (7) would also disappear—so it is only a question of definition, leading to the same results). The sign $(-1)^{k+l}$ in equation (9) has its origin in reversing the laboratory frame: $H^{kl}(-r, \hat{s}_1, \hat{s}_2) = (-1)^{k+l} H^{kl}(r, \hat{s}_1, \hat{s}_2)$. The non-orthogonality of basis orbitals may be simply taken into account by replacing the transfer element V by $V - ES$ (the transfer element reduced by energy times overlap) in the SSCA/EMA equations [3, 31]. The density of states of the multiband system including the non-orthogonality is given by

$$D(E) = -\frac{1}{\pi} \Im \left[\sum_k (2k+1)\bar{G}^k + \sum_{k,l,\mu} 4\pi\rho(2l+1)\bar{G}^l \int_0^\infty H_{lk\mu}(r)(2k+1)\bar{G}^k (-1)^{k+l} S_{kl\mu}(r)r^2 dr \right] \quad (10)$$

where all energy-dependent terms on the rhs are to be taken at energies with an infinitesimally small positive imaginary part.

3. Liquid silicon

The pair distribution for the following calculations of the electronic density of states of liquid silicon was taken from the experimental data of Waseda *et al* [32] obtained at a temperature of $T = 1733$ K. For the mass density we use $\rho_m = 2.59 \text{ g cm}^{-3}$ [33].

First, we consider the simple sp^3 model with the Slater–Koster parameters from Goodwin *et al* [34]. We have used a (one-dimensional) grid for the distance of atoms R at $N = 4096$ points equally spaced by $\Delta R = 0.05 a_B$ (a_B : Bohr radius). The total density of states is shown in figure 1 together with analogous tight-binding molecular dynamics results from Wang *et al* [22] and López-Martín *et al* [24]. For comparability, we shifted (if necessary) all curves in such a way that the Fermi energy E_F is at 0 eV. As pointed out by López-Martín *et al*, the density of states in the SSCA/EMA fits very well with molecular dynamics results for the same Slater–Koster parameters. That is true even if we use the experimental pair distribution function instead of that from the MD simulation. No principal differences occur in the DOS on such a modification of the distribution function [35]. Comparing the results of the sp^3 model with plane-wave calculations (see figure 2) some fundamental deviations occur:

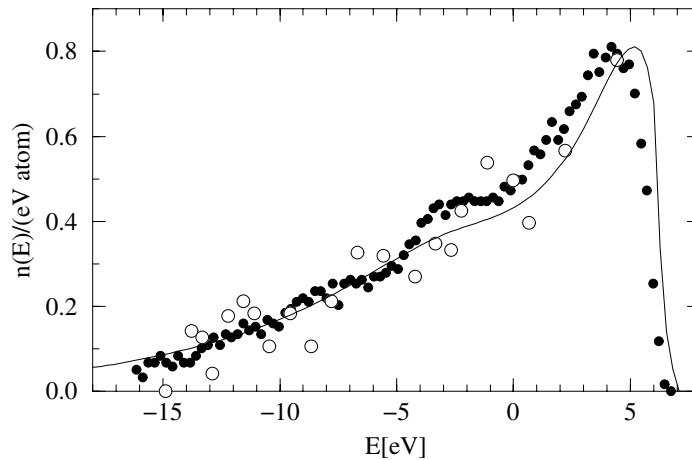


Figure 1. The total density of states of liquid silicon in the SSCA/EMA within the sp^3 model (—) compared to tight-binding MD results: from López-Martín *et al* [24], ●, and from Wang *et al* [22], ○.

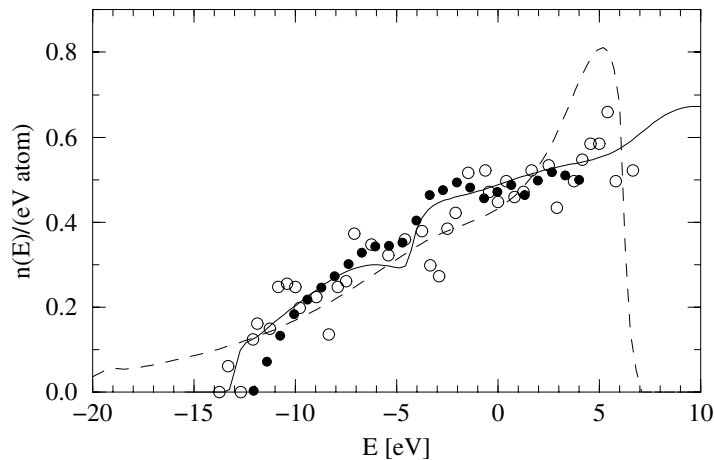


Figure 2. The total density of states of liquid silicon calculated with the SSCA/EMA within the sp^3 model (- - -) and the sp^3d^5 model (—) compared to plane-wave MD results from Štich *et al* [7], ○, and Jank and Hafner [15], ●.

- (a) First, the lower band edge is placed several eV lower in the sp^3 model relative to the Fermi energy.
- (b) Second, the density of states of the sp^3 model near the Fermi level shows a very non-metallic behaviour with a concave increase ending in a relatively sharp peak of p-like orbitals whereas the plane-wave results show the typical metallic \sqrt{E} -dependence.

These failings will lead to unsatisfactory results for other physical (e.g., optical) properties. But not only properties of excited states are affected by the unrealistic behaviour of the sp^3 model—so also are electronic ground-state properties like the pressure dependence of the density. This is not surprising because Goodwin *et al* [34] already noted that their parameter set leads to worse results for the denser phases of silicon. Klein *et al* [20] showed that by using the (non-

orthogonal) spd basis of Frauenheim *et al* very reasonable results for the pressure dependence of the density are obtained. Therefore, we use the same parameters [36] for a calculation of the electronic density of states within the SSCA/EMA. Since the data are given on a grid spaced by $\Delta R = 0.02 a_B$ we now use 8192 points. With this non-orthogonal spd basis set the agreement with plane-wave calculations becomes excellent (figure 2). The width of the lower part up to the Fermi energy fits well. Also, the shape with a mainly \sqrt{E} -character and the dip at ≈ 5 eV below the Fermi energy are well reproduced. This dip corresponds to the separation between the mainly p-like and the sp^3 hybridized orbitals in the density of states of crystalline silicon whereas the gap between the sp^3 hybridized and the s-like orbitals vanishes totally. At the Fermi level there is no dip at all, so we conclude that the minimum found in [20] can only be of statistical nature.

Not only the total density of states but also the partial densities fit very well to the ones obtained by plane-wave calculations [15] (figure 3). Note that the orbital quantum numbers are not conserved in the whole system and, especially at higher energies, the distribution into partial densities is not definite. Nevertheless, it is clearly seen that the part of the orbitals containing d-like symmetry does not vanish below the Fermi energy. A fraction of about 0.35 of the four valence electrons have d character. This amount is very similar to the d part found in the solid state [37]. The distribution of the remaining valence electrons into s and p states corresponds also to that of solid silicon.

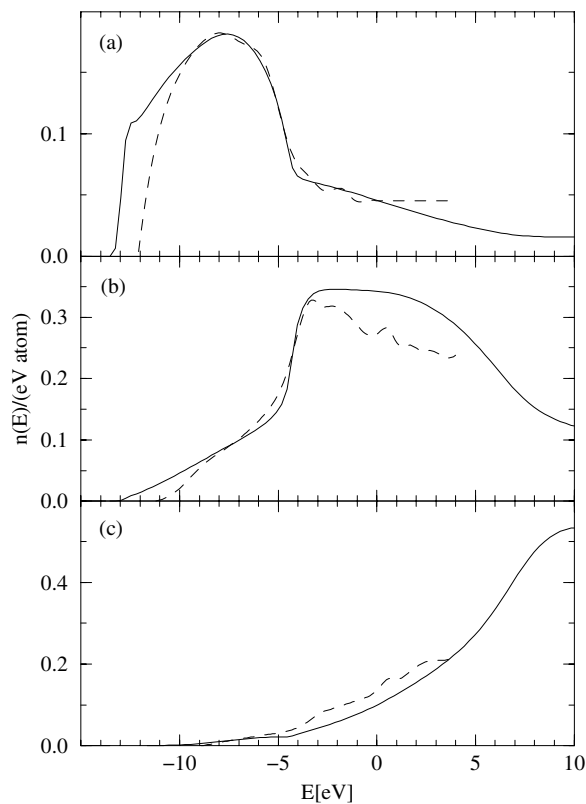


Figure 3. Partial densities of (a) s-like states, (b) p-like states and (c) d-like states of liquid silicon in the SSCA/EMA within the sp^3d^5 model (—) compared to plane-wave MD results from Jank and Hafner [15] (- - -).

4. Conclusions

We extended the molecular fluid approach to the sp^3 liquid of Lomba *et al* to arbitrarily high orbital quantum numbers. This generalization enables us to combine the advantages of integral equation methods like the SSCA/EMA (i.e., less computational effort than in MD or MC simulations and no statistical errors) with more complete basis sets. We performed SSCA/EMA calculations for liquid silicon both as an sp^3 liquid and as an sp^3d^5 liquid. Comparison of the sp^3 model with plane-wave calculations shows both deviations in the unoccupied part of the density of states and a broadened density of valence states. In contrast to this, the results from the sp^3d^5 model agree very well with the plane-wave calculations in the valence regime as well as over a wide range of the conduction band. Taken as a supplement to MD calculations, the absence of statistical errors in the SSCA/EMA allows us to conclude that the slight dip sometimes found at the Fermi energy is an artifact.

Acknowledgments

The author would like to thank Professor H M Urbassek for helpful comments and Dr B Hüttner and Dr M Brieger for careful reading of the manuscript.

References

- [1] Ishida Y and Yonezawa F 1973 *Prog. Theor. Phys.* **49** 731
- [2] Movaghar B, Miller D E and Bennemann K H 1974 *J. Phys. F: Met. Phys.* **4** 687
- [3] Roth L M 1973 *Phys. Rev. B* **7** 4321
- [4] Kresse G 1996 *J. Non-Cryst. Solids* **205–207** 833
- [5] Chelikowsky J R, Troullier N and Binggeli N 1994 *Phys. Rev. B* **49** 114
- [6] Silvestrelli P L, Alavi A, Parrinello M and Frenkel D 1997 *Phys. Rev. B* **56** 3806
- [7] Štich I, Car R and Parrinello M 1991 *Phys. Rev. B* **44** 4262
- [8] Godelevsky V V, Derby J J and Chelikowsky J R 1998 *Phys. Rev. Lett.* **81** 4959
- [9] Godelevsky V V and Chelikowsky J R 1998 *J. Chem. Phys.* **109** 7312
- [10] Silvestrelli L and Parrinello M 1998 *J. Appl. Phys.* **83** 2478
- [11] Sprink M, Hutter J and Parrinello M 1996 *J. Chem. Phys.* **105** 1142
- [12] Röhrlisberger U and Parrinello M 1997 *J. Chem. Phys.* **106** 4658
- [13] Broughton J Q and Li X P 1987 *Phys. Rev. B* **35** 9120
- [14] Ishimaru M, Yoshida K, Kumamoto T and Motooka T 1996 *Phys. Rev. B* **54** 4638
- [15] Jank W and Hafner J 1990 *Phys. Rev. B* **41** 1497
- [16] Omote K and Waseda Y 1996 *Japan. J. Appl. Phys.* **35** 151
- [17] Petkov V 1995 *J. Phys. Chem.* **7** 5745
- [18] Venkatesh R 1995 *Indian J. Pure Appl. Phys.* **33** 236
- [19] Kim E and Lee Y H 1994 *Phys. Rev. B* **49** 1743
- [20] Klein P, Urbassek H M and Frauenheim T 1999 *Comput. Mater. Sci.* **13** 252
- [21] Virkkunen R, Laasonen K and Nieminen R M 1991 *J. Phys.: Condens. Matter* **3** 7455
- [22] Wang C Z, Chang C T and Ho K M 1992 *Phys. Rev. B* **45** 12 227
- [23] Aloisio M-A, Singh V A and Roth L M 1981 *J. Appl. Mech.* **11** 1823
- [24] López-Martín J-L, Lomba E, Kahl G, Winn M D and Rassinger M 1997 *J. Phys.: Condens. Matter* **9** 3321
- [25] Ching W Y 1990 *J. Am. Ceram. Soc.* **73** 3135
- [26] Lomba E, López-Martín J L and Kahl G 1996 *J. Chem. Phys.* **105** 7735
- [27] Logan D E and Winn M D 1988 *J. Phys. C: Solid State Phys.* **21** 5773
- [28] Blum L 1972 *J. Chem. Phys.* **56** 303
- [29] Lado F 1982 *Mol. Phys.* **47** 283
- [30] Edmonds A R 1996 *Angular Momentum in Quantum Mechanics* (Princeton, NJ: Princeton University Press)
- [31] Chen Z and Stratt R M 1991 *J. Chem. Phys.* **94** 1426
- [32] Waseda Y, Shinoda K, Sugiyama K and Takeda S 1995 *Japan. J. Appl. Phys.* **34** 4124

- [33] Waseda Y 1980 *The Structure of Non-Crystalline Materials; Liquids and Amorphous Solids* (New York: McGraw-Hill)
- [34] Goodwin L, Skinner A J and Pettifor D G 1989 *Europhys. Lett.* **9** 701
- [35] Lomba E, López-Martín J L and Anta J A 1997 *J. Chem. Phys.* **106** 10238
- [36] Sieck A and Frauenheim T 1999 Nonorthogonal spd Slater–Koster parameters of silicon, personal note from P Klein
- [37] Rohr G C 1999 Decomposed density of states of silicon, personal note